Absorption and CD Spectroscopy and Modeling of Various LH2 Complexes from Purple Bacteria

Sofia Georgakopoulou,* Raoul N. Frese,* Evelyn Johnson,[†] Corline Koolhaas,[‡] Richard J. Cogdell,[†] Rienk van Grondelle,* and Gert van der Zwan[‡]

*Department of Biophysics and Physics of Complex Systems, Vrije Universiteit, 1081 HV Amsterdam, The Netherlands; [†]Division of Biochemistry and Molecular Biology, University of Glasgow, Glasgow G12 8QQ, United Kingdom; and [‡]Department of Analytical Chemistry and Applied Spectroscopy, Vrije Universiteit, 1081 HV Amsterdam, The Netherlands

ABSTRACT The absorption (OD) and circular dichroism (CD) spectra of LH2 complexes from various purple bacteria have been measured and modeled. Based on the lineshapes of the spectra we can sort the LH2 complexes into two distinguishable groups: "acidophila"-like (type 1) and "molischianum"-like (type 2). Starting from the known geometric structures of *Rhodopseudomonas* (*Rps.*) *acidophila* and *Rhodospirillum* (*Rsp.*) *molischianum* we can model the OD and CD spectra of all species by just slightly varying some key parameters: the interaction strength, the energy difference of α- and β-bound B850 bacteriochlorophylls (BChls), the orientation of the B800 and B850 BChls, and the (in)homogeneous broadening. Although the ring size can vary, the data are consistent with all the LH2 complexes having basically very similar structures.

INTRODUCTION

The photosynthetic purple bacteria are a widely studied group of photosynthetic bacteria. Although a high diversity is found among the species with respect to growth conditions, habitats, and cellular shape, the photosynthetic apparatuses of all species are quite similar. The two most striking characteristics of the pigment-protein complexes involved in bacterial photosynthesis are the highly symmetric arrangement of the subunits within the antenna complexes, and the supramolecular organization of the complexes as a whole, together with the largest redshift of the absorption band of the pigments found in any photosynthetic organism (Van Grondelle et al., 1994; Zuber and Cogdell, 1995; Pullerits and Sundström, 1996; Sundström et al., 1999).

The photosynthetic apparatus of all purple bacteria consists of a light-harvesting complex (LH1) to absorb incoming photons, a reaction center (RC) where the primary charge separation takes place, and a cyclic electron transfer chain involving cytochrome *c*, the cytochrome *bc*$_1$ complex, and a quinone by which the original charge separation is converted into a stable transmembrane electrochemical potential (Shinkarev and Wraight, 1993). For the RC and cyt*bc*$_1$ complex a structural model exists to atomic resolution (Xia et al., 1977; Deisenhofer et al., 1985; Iwata et al., 1998). From low-resolution cryomicroscopic data a structural model was proposed for LH1 and the LH1-RC complexes (Karrasch et al., 1995). Recently we have reported the long-range order of the RC-LH1-cyt*bc*$_1$ complexes within the membrane of *Rhodobacter* (*Rb.*) *sphaeroides*

when the PufX gene is expressed (Frese et al., 2000). A similar long-range order was proposed from electron microscopy results on the same LH1-RC-containing membrane (Walz et al., 1998; Jungas et al., 1999). These supercomplexes are all aligned in regular arrays on a cylindrical membrane with a specific orientation of the RC with the LH1 ring. The orientation is found to be such that the transition dipole moment of the lowest Q_y transition of the special pair is almost perpendicular to the long axis of the membrane (Frese et al., 2000).

Some purple bacterial species have the ability to synthesize another light-harvesting antenna to increase the absorption of sunlight: light-harvesting complex 2 (LH2). The ratio of RC/LH1 complexes in the membrane is always fixed, but the amount of LH2 complexes is strongly dependent on the growth conditions (Aagaard and Sistrom, 1972). Structural data to atomic resolution exist for two such complexes: LH2 of *Rhodopseudomonas* (*Rps.*) *acidophila* and *Rhodospirillum* (*Rsp.*) *molischianum* (McDermott et al., 1995; Freer et al., 1996; Koepke et al., 1996). The LH2 complex from *Rps. acidophila* demonstrates a high (ninefold) symmetry and consists of two pigment rings: one in the hydrophilic part of the complex, which absorbs at 800 nm and is therefore called the B800 ring, and the other in the hydrophobic part of the complex with a main absorption band at 850 nm, called the B850 ring. The B800 ring has a diameter of 31 Å and consists of nine BChls, each bound to an α-helical transmembrane (α) apoprotein. These α-helices, of 23 residues each, are closely packed side by side and form an inner cylinder of radius 18 Å. Another nine (β) apoproteins are situated radially with respect to the α-apoproteins and form an outer cylinder of radius 34 Å. A pair of the α and β proteins are known as the $\alpha\beta$-heterodimer. Forming the outer wall of the complex, the B800 BChls are placed between the β-apoproteins, with their chlorin planes almost parallel to the plane of the total ring. The α- and β-apoproteins each contain a conserved histidine in the

transmembrane stretch. The $\alpha\beta$-heterodimer then binds the BChls. The nine BChl dimers form the more tightly coupled B850 ring. The chlorin planes of the B850 BChls are more or less perpendicular to the plane of the membrane. Furthermore, within the $\alpha\beta$-heterodimer, the orientations of the Q_y transitions are antiparallel and almost transversal to the ring, while the Q_x transitions are approximately parallel to the symmetry axis of the total ring. In the entire LH2 complex carotenoids are present in a 1:3 ratio to BChl.

The crystal structure of the LH2 complex of *Rsp. molischianum* is very similar to that of *Rps. acidophila* (Koepke et al., 1996). Again, the entire complex shows a high symmetry, which this time, however, is eightfold. The $\alpha\beta$-heterodimers are, as before, circularly arranged, but in this case they are somewhat more densely packed, thus creating an even tighter distribution of the B850 BChls and slightly higher interaction energies between the pigments. In the transmembrane region, both structures are very similar. The major difference between the two complexes lies in the orientation of the B800 BChls. Although the B850 BChls of *Rsp. molischianum* have more or less the same orientation as those of *Rps. acidophila*, this is not the case for the B800 BChls. Here, the chlorin planes are tilted compared to the corresponding chlorins of the *Rps. acidophila* complex, by ~20°, with a further rotation by 90° around their own symmetry axis. The two LH2 complexes also differ in the carotenoid molecules which, however, have the same orientations in both structures with only minor deviations close to the B850 BChls.

Earlier CD studies of purple bacterial antenna systems indicate that the types of LH2 complexes found can vary greatly (Cogdell and Scheer, 1985). Here we report the results of a comprehensive comparison study by means of absorption and circular dichroism spectroscopy of LH2 complexes from many different species. These spectra indicate that we can distinguish two separate groups of LH2 complexes: *acidophila*-like and *molischianum*-like. Recently, we and others have been able to relate the structural data of the LH2 complex taken from *Rps. acidophila* to its OD and CD spectra (Sauer et al., 1996; Koolhaas et al., 1997a, 1998; Linnanto et al., 1999). Important features of the CD spectra could be modeled satisfactorily. First of all, the signs of the CD bands and their relative magnitude both depend strongly on the orientation and the excitonic interaction energy. Second, the redshift of the zero crossing of the B850 CD lines compared to the absorption maximum can be modeled by introducing an energy mismatch between the α- and β-bound BChls, and taking interactions into account between all the pigments in the ring. One other important feature expected from the afore-mentioned model is a transition with some dipolar and rotational strength of the B850 high-energy exciton band below 800 nm. This transition is indeed detected, as we have shown in Koolhaas et al. (1998), and its position indicated a nearest-neighbor interaction energy of ~250–300 cm^{-1}, in agreement with

estimates based on pump-probe spectra (Pullerits et al., 1996; Novoderezhkin et al., 1999), superradiance (Monshouwer et al., 1997), and quantum chemical calculations (Alden et al., 1997; Hu et al., 1997; Cory et al., 1998; Krueger et al., 1998; Scholes et al., 1999; Tretiak et al., 2000). We now show that we can obtain similar satisfactory results for the LH2 complex of *Rsp. molischianum* and, by slightly changing some key parameters, for all LH2 complexes investigated. Our results show that the observed variation in the spectra can be explained on the basis of the model calculations, and furthermore that there only appear to be two fundamental types based on either the *molischianum* or the *acidophila* structure. The main difference between these two types lies not in the symmetry number of the ring, but in the orientation of the B800 pigments.

MATERIALS AND METHODS

Cells of *Rps. acidophila* strains 10050 (high light, HL), 7750 (HL, and low light, LL), *Rps. palustris* (HL and LL), *Rps. cryptolactis* (HL), *Chromatium (Cm.) vinosum* strain D (HL), *Cm. purpuratum* (HL), *Rsp. molischianum* (HL), *Rhodobacter (Rb.) sphaeroides* strain G1C and 2.4.1 (both HL), and *Rubrivivax (Ru.) gelatinosus* (HL), were grown anaerobically in light as previously described (Cogdell and Thorber, 1979; Cogdell et al., 1983, 1990a; Cogdell and Crofts, 1990b; Evans et al., 1990; Halloren et al., 1995). The cells were harvested by centrifugation, resuspended in 20 mM Tris HCl pH 8.0, and disrupted by passage through a French press at 7 MPa. The photosynthetic membranes were then pelleted by centrifugation (Cogdell and Hawthornthwaite, 1993) and resuspended in 20 mM Tris HCl to give an OD at their NIR absorption maximum of 50. The required antenna complexes were isolated and purified as previously described (Cogdell and Hawthornthwaite, 1993). The basic procedure involves solubilization with 1% v/v LDAO, fractionation of LH1 from LH2 by sucrose density centrifugation, and followed by further purification by ion exchange chromatography on DEAE cellulose. The integrity of the antenna samples was routinely checked spectrophotometrically.

The samples were diluted in a buffer with a final concentration of 20 mM Tris HCl, pH 8.2. This buffer also contains 0.1% *N,N*-dimethyldodecylamine-*N*-oxide (LDAO) as detergent. For the low-temperature measurements, glycerol concentrations of 70% (v/v) were used to obtain transparency of the samples upon cooling. The samples were diluted to an OD of 0.5–0.6 cm^{-1}. For the low-temperature measurements a special home-built cuvette with removable windows was used, to be attached to the cuvette with some grease. Thus the sample does not overflow the cuvette while being cooled, and it remains homogeneous and transparent. For the low-temperature measurements the cuvette is placed in an Oxford Instruments DN1704 liquid nitrogen cryostat.

RESULTS

Absorption and CD spectra of LH2 complexes were taken from the following species: *Rps. acidophila* (strain 10050, HL), *Rps. acidophila* (strain 7750, HL), *Rps. acidophila* (strain 7750, LL), *Rps. palustris* (HL), *Rps. palustris* (LL), *Rps. cryptolactis*, *Cm. vinosum*, *Cm. purpuratum*, *Rsp. molischianum*, *Rb. sphaeroides* (strains G1C and 2.4.1), and *Ru. gelatinosus*. Most preparations were measured at 77 K and at room temperature (RT), and some with different detergent concentrations (see Discussion). In Figs. 1–4 we
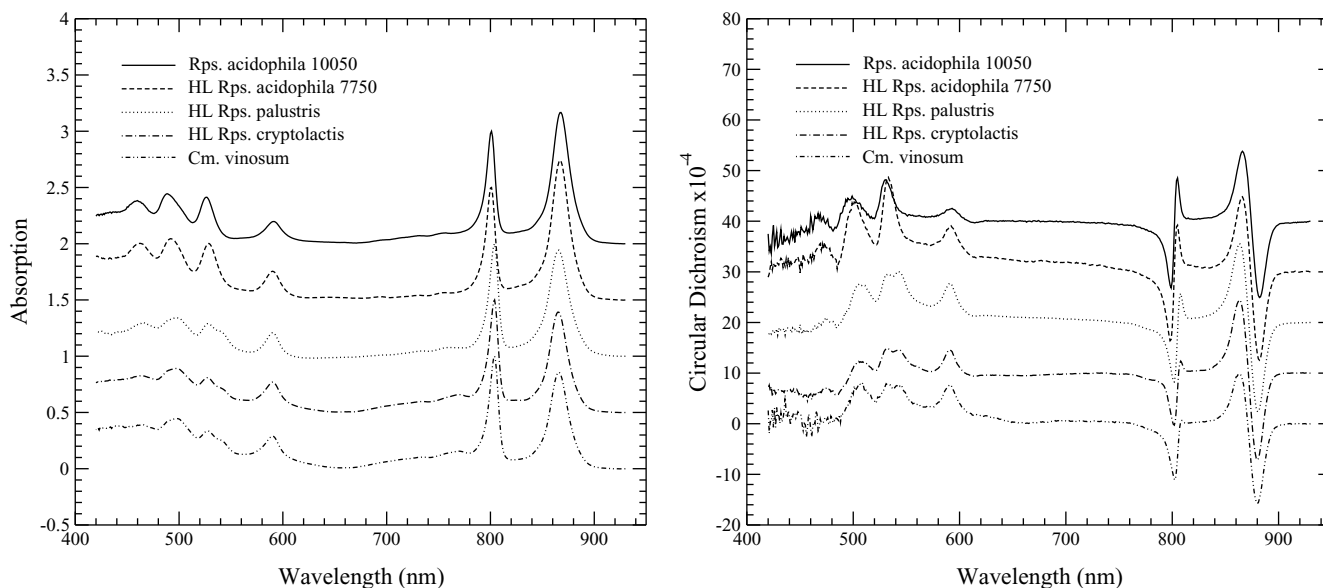
FIGURE 1 Experimental 77 K absorption (*left*) and CD spectra (*right*) of the four antenna species belonging to type 1. The baseline of the spectra was shifted by 0.5 units (0) or 10 units (CD) to improve distinguishability in the 800–850-nm range. All spectra were scaled to an absorption of 1 at the maximum of the B800 absorption peak.

show the 77 K absorption and CD spectra of all LH2 complexes. Although our analysis concentrates on the 800–850 nm range of these spectra, they also have well-resolved bands in the Q_x region (around 600 nm), and of the carotenoid bands (below 550 nm).

The general properties of the spectra in the 800–850-nm range are as follows: all absorption spectra exhibit two pronounced peaks, one in the 800-nm range, and one around 860 nm, where the width of the 860 absorption peak is generally about twice that of the 800 band. The CD spectra show more variation. Going from the blue to the red we first encounter the 800 band, of which the signature can vary, and also the peak ratio. In a number of cases sub-bands can also be identified. The 850-nm region is more consistent, although here also the peak ratio can vary. The most notable feature of the 850 band is the redshift of the zero crossing of the CD spectrum with respect to the absorption maximum of ~6 nm, which was shown to be an indication of a ring-like structure, and an excitation energy difference between the α- and β-bound pigments (Koolhaas et al., 1997a). Although we report the spectra of *Rps. palustris* (LL) and *Cm. purpuratum* (cf. Fig. 4), these spectra will not be used further for modeling.

Rps. palustris (LL) differs from *Rps. palustris* (HL) in its growth conditions, particularly the light intensity. The positions of the bands are similar for the HL and the LL species, but the magnitude ratio between the B800 and the B850 band is 3.3 times smaller in the LL species. The full-width at half-maximum (FWHM) of the two absorption bands follows the pattern of those of the other complexes: the B800 band has a FWHM of 15 nm, and the B850 band

of 26 nm. The CD spectrum appears to be quite different; it does not have two pairs of lines as usual, but we can also identify a fifth negative line between the B800 and B850 pairs, approximately at 816 nm. In addition, the positive B850 line is very wide and small in magnitude. The zero crossing of the B800 and B850 band signals does not differ much from what we have seen so far, indicating that we are
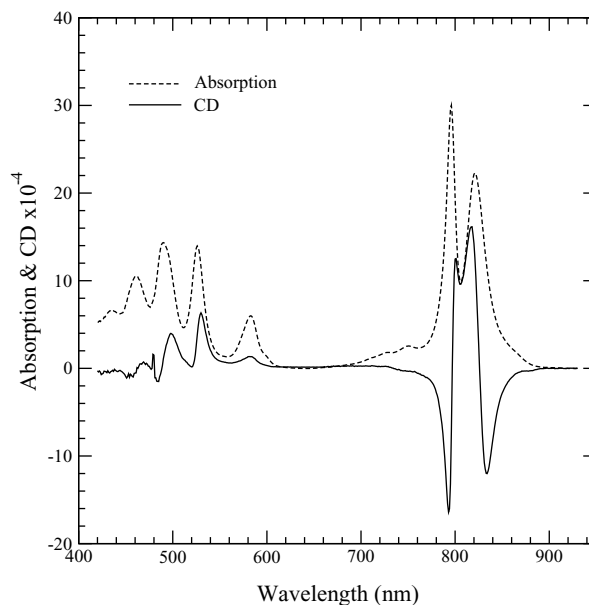

FIGURE 2 Experimental 77 K absorption and CD spectra of LL *Rps. acidophila* (strain 7750). The absorption spectrum was multiplied by a factor of 30, to show OD and CD in one figure.
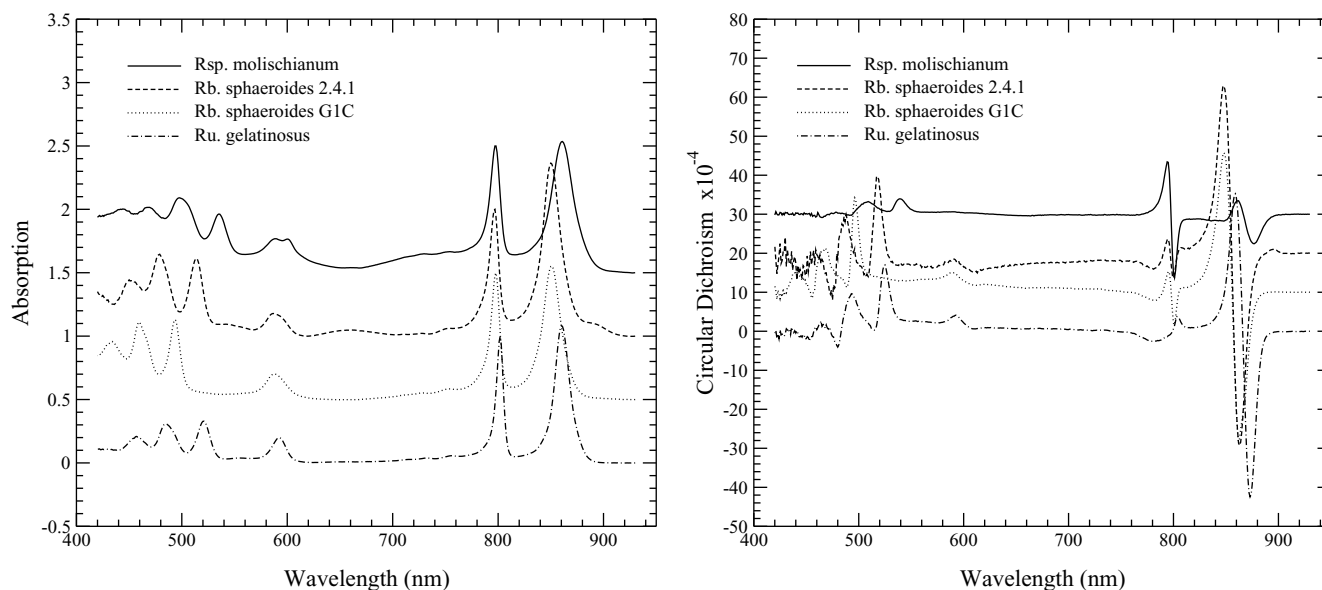
FIGURE 3   Experimental 77 K absorption (*left*) and CD spectra (*right*) of the four antenna species belonging to type 2. The baseline of the spectra was shifted by 0.5 units (0) or 10 units (CD) to improve distinguishability in the 800–850-nm range.

very likely still dealing with a ring-like structure. A small positive band can be clearly distinguished at 767 nm, and a shoulder on the negative B800 CD signal at 769 nm, i.e., ~10 nm more to the blue than for the other complexes. The low-light form of *Rps. palustris* is likely to be a mixture of different forms, as under low light conditions up to four different variants of the β-apoprotein can be expressed (Tharia et al., 1999), and it is unclear what the spectroscopic properties, such as excitation energies, of the BChls bound

to these proteins are. Furthermore, it is unclear whether each antenna contains only one form of the β protein, or is itself a mixture.

Cm. purpuratum is a B800–830 complex (sometimes referred to as LH3). The CD signal of *Cm. purpuratum* is exceptionally large in the 830-nm area. Such a strong CD signal has not been observed before, and may reflect larger angles of the transition dipoles with the ring plane (cf. Modeling the Spectra). However, in the 800-nm area the CD
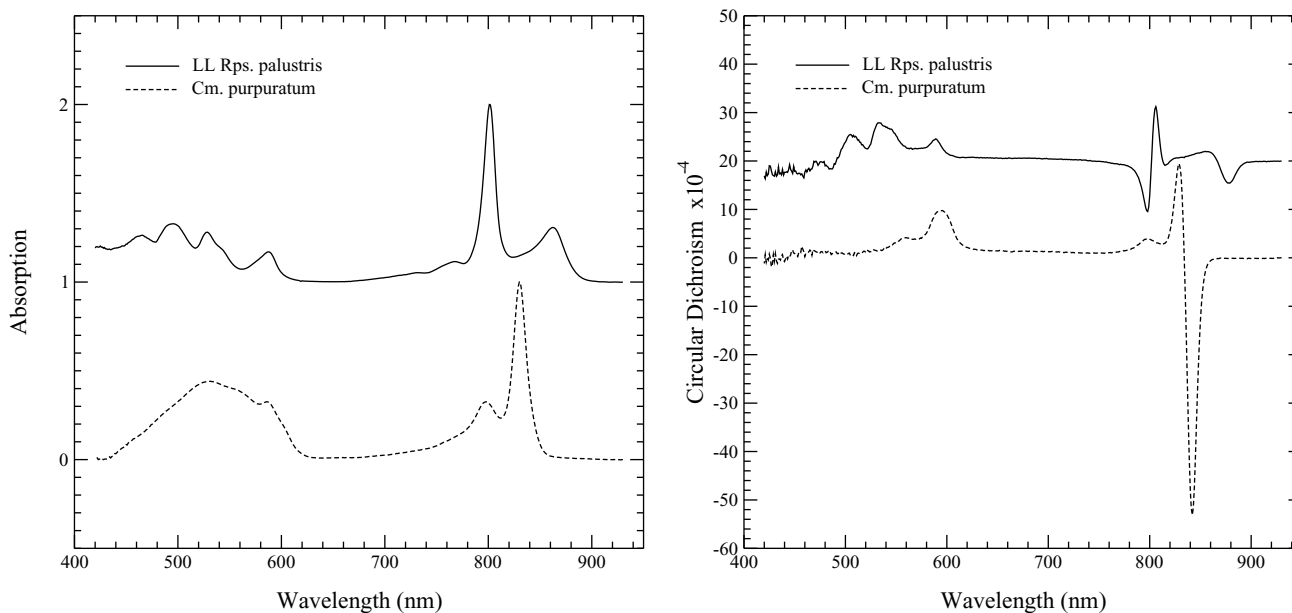

FIGURE 4   Experimental 77 K absorption (*left*) and CD spectra (*right*) of the two species *Rps. palustris* (LL) and *Cm. purpuratum*.

signal features only a small positive band, and not a pair of lines. This band is five times smaller than the positive line at 830 nm. The redshift of the zero crossing with respect to the absorption maximum at 830 nm is 4 nm, again an indication of a ring-like structure. This is the smallest redshift observed so far. In the 800-nm area the small positive CD band has a maximum at 798 nm, exactly at the same point as the absorption maximum. No other features can be distinguished in these spectra in the Q_y region. Some parameters derived from the spectra of these species are collected in Table 1.

Based on the position and lineshapes of the OD and CD spectra in the 800-nm and the 850-nm regions, two further categories can be distinguished. The first category contains those complexes with OD and CD spectra similar to the LH2 complex of *Rps. acidophila* (strain 10050, HL). The complexes similar to *Rsp. molischianum* form the second category.

Type 1 complexes

The first group (type 1) consists of LH2 complexes from *Rps. acidophila* (strain 10050, HL), *Rps. acidophila* (strain 7750, HL), *Rps. palustris* (HL), *Rps. cryptolactis*, and *Cm. vinosum*. The spectra all show as prominent features that remain similar throughout: 1) positions of the absorption maxima of the B800 and B850 bands; 2) positions of the maxima and minima, and redshift of the zero crossing relative to the absorption maxima of the B850 CD band

of ~6 nm; and 3) the overall shape and signature of the CD bands. Relevant parameters of all the spectra (also those of the room temperature spectra not shown) are listed in Table 1.

The absorption spectra of all type 1 LH2 complexes show the two typical bands, the B800 and the B850 band. The B800 band originates from the nine weakly interacting BChls in the B800 ring, whereas the B850 is the result of the stronger excitonically coupled 18 BChls in the B850 ring. For all the type 1 complexes, the maxima of these bands are situated around 802 nm and 866 nm, respectively, at 77 K. In all cases, except *Rps. cryptolactis* (HL), the FWHM of the B800 band is half that of the B850 band, 11 and 22 nm, respectively. For *Rps. cryptolactis* (HL) the values are 11 and 29 nm. A minor difference is in the absorption maxima of both bands: the two *Rps. acidophila* complexes have a slightly larger B850 maximum, all other complexes have a higher B800 peak.

In all absorption spectra a small sideband is observed on the blue side of the B800 absorption band, of which the exact position varies between the species, between 760 and 770 nm. We have shown before (Koolhaas et al., 1997a, 1998), that due to Davidov splitting, a high exciton component of the B850 band can acquire some oscillator strength in the 800-nm region. The small band, however, is too far to the blue, and in addition appears to be uncorrelated with the position of the B850 band to be the high exciton component of this band. The origin of the small

TABLE 1   Prominent features of the OD and CD spectra of all complexes studied

Complex	OD (nm)	CD (nm)	B850	CD ratio
Type 1				
Rps. acidophila (10050), 77K	801 (11); 867 (22)	802; 874	1.16	−0.9:0.6:1:−1.1
Rps. acidophila (7750), 77K	801 (11); 867 (22)	802; 874	1.25	−0.9:0.6:1:−1.2
Rps. acidophila (10050), RT	801 (22); 856 (29)	863	1.49	−0.56:0:1:−0.96
Rps. acidophila (LL) 77K	795 (13); 821 (23)	796; 825	0.74	−1.01:0.76:1:−0.76
Rps. palustris (HL), 77K	804 (11); 866 (22)	806; 872	0.94	−0.8:0.4:1:−1.2
Rps. palustris (HL), RT	803 (22); 858 (32)	865	1.21	−0.53:0:1:−1.2
Rps. cryptolactis (HL), 77K	804 (11); 865 (29)	807; 872	0.90	−0.7:0.2:1:−1.2
Rps. cryptolactis (HL), RT	803 (26); 858 (32)	865	1.34	−0.52:0.1:1:−0.64
Cm. vinosum, 77K	804 (11); 866 (22)	808; 872	0.86	−1.1:0.06:1:−1.6
Cm. vinosum, RT	803 (22); 855 (32)	861	1.02	−0.56:0:1:−0.94
Type 2				
Rsp. molischianum, 77K	797 (13); 861 (26)	798; 867	1.04	3.7:−4.6:1:−2.1
Rb. sphaeroides (G1C), 77K	798 (11); 851 (22)	800; 856	1.04	0.1:−0.2:1:−1.1
Rb. sphaeroides (2.4.1), 77K	797 (11); 850 (22)	798; 856	1.40	0.1:−0.2:1:−1.2
Ru. gelatinosus, 77K	802 (9); 860 (18)	866	1.1	0.1:0:1:−1.2
Ru. gelatinosus, RT	803 (22); 855 (29)	860	1.48	0:0:1:−1.03
Rps. palustris (LL), 77K	801 (15): 862 (26)	802; 867	0.3	−5.2:5.5:1:−2.2
Rps. palustris (LL), RT	803 (32); 853 ()	862	0.45	−1.9:2.4:1:−0.78
Cm. purpuratum 77K	798 (29); 830 (18)	834	3.0	0.2:0:1:−2.7
Cm. purpuratum RT	800 (); 827 (39)	827	2.06	0:0:1:−5.1

OD: positions of the maxima of the two major bands in the absorption spectrum, and their FWHM (in parentheses). CD: positions of the zero-crossings of the CD signal in the B800 and B850 band, respectively. B850: B850 maximum scaled with respect to the B800 maximum. CD ratio: maxima/minima of the CD spectrum, from the blue to the red, scaled with respect to the positive (blue) B850 CD intensity.

band could be free BChl, but more likely it is a higher vibronic transition (Reddy et al., 1991).

The CD spectra of the type 1 complexes all consist of two pairs of lines with the signature pattern $-++-$. The lines in the 850-nm range are quite symmetric, with a zero crossing that is 6–7-nm redshifted with respect to the 850-nm absorption maximum. In the 800-nm range the CD spectrum has a large negative peak, and a positive peak of varying magnitude, which is the result of overlapping contributions due to the B800 band and the high exciton component of the B850 band. These results suggest that there is a strong similarity between the LH2 systems of these bacteria, which is confirmed by the model calculations given below.

Type 2 complexes

This group consists of *Rsp. molischianum*, *Rb. sphaeroides* (strains G1C and 2.4.1), and *Ru. gelatinosus*. The absorption bands of the pigment complexes of these bacteria are not significantly different from those of the first group, in all cases the width of the 800-nm peak is half that of the B850 peak, and the energy splitting between the bands is again between 50 and 60 nm. The difference is in the CD spectra. The major similarity that characterizes the members of this group is the reversal of the B800 CD signal compared to the *acidophila* type CD spectra. The signs of the CD lines are in this case with increasing wavelength, $+-+-$. Parameters found from these spectra are also collected in Table 1.

Although the spectra of *Rsp. molischianum* and *Ru. gelatinosus* differ in the relative magnitudes of the CD, *Ru. gelatinosus* differs with just one positive line in the B800 CD signal and a wide negative band, and *Rsp. molischianum* has a relatively small 850-nm CD signal, we will show in the Modeling section that the spectra can all be derived from the *Rsp. molischianum* structure by relatively small changes of the angles of the B800 pigments. This, in conjunction with the signature of the CD lines, justifies putting these four systems in one group.

The redshift of the CD zero crossing with respect to the absorption maximum in the 850-nm region is in all cases ~6 nm, very similar to that of the type 1 LH2's. The position of the B850 band maximum of the type 1 spectra has a mean value of around 866 nm, while for the second group this is 856 nm. The distance between the 800 and 850 peak is marginally smaller in the type 2 spectra, but because the 800-nm band overlaps the high-exciton band of the B850 pigments, we cannot draw any definite conclusions regarding the interaction strength between the B850, which we expect to be slightly larger in the *Rsp. molischianum* type than in the *Rps. acidophila* type.

Effects of temperature and detergent

As mentioned before, the spectral properties of LH2 complexes are sensitive to temperature (Wu et al., 1997) and

detergent concentration. The temperature effect is most considerable for the B850 band, a >15-nm redshift of the absorption maximum by lowering the temperature from RT to 77 K. The B800 band can be attenuated strongly by detergent. It is known that the B800 band can be titrated fully away by LiDS, to reappear again when the detergent is flushed out (Clayton and Clayton, 1981). The amount of LDAO, a commonly used detergent in buffers, also affects the B800 band, not so much in absorption but considerably for the CD lines.

Type 1 and type 2 species have the B850 CD zero crossing following the temperature shift of the absorption maximum. For the other complexes, that is not the case; LL *Rps. palustris* has an absorption maximum band at 853 at RT and at 862 at 77 K, while the CD zero crossing moves from 862 to 867 nm. *Cm. purpuratum* has an absorption maximum shift of only 3 nm, but a 7-nm shift of the CD crossing. In contrast to the B850 band, the B800 band of all species hardly shifts with temperature. The most striking difference between RT and 77 K spectra of this band is the shape of the CD signal; at RT the positive line vanishes. The same effect is also observed in 77 K spectra when the detergent concentration is lowered. In both cases the absorption bands become much wider, which can be the direct cause of the vanishing of the positive line in the CD; the overlap between the positive and negative line increases, thus diminishing the signal. In addition to the line-broadening effect at higher temperatures due to larger disorder, another effect could arise from "shrinkage" of the protein upon lowering the temperature. Then pigments get closer together, inducing a further redshift. The closer the pigments are, the less effect lowering the temperature should have. Indeed, type 1 complexes appear to shift further than type 2.

The implication of such shrinkage is that the pigments move closer together, thus increasing the interaction strength, and consequently the distance between the high and low exciton components of the B850 band would move further apart. A similar effect was measured by increasing the pressure (Freiberg et al., 1994; Wu et al., 1997; Rätsep et al., 1998).

For all LH2s the B800 band is in a rather stable position with changing temperature. The corresponding CD zero crossings of the B800 CD signal has only a 1-nm shift to the red in the case of *Rsp. molischianum* and *Rb. sphaeroides* (strain 2.4.1), and 2 nm for the other *sphaeroides* complex.

Modeling the spectra

Extensive descriptions of the modeling procedures used can be found in Koolhaas et al. (1997a, b; 2000). Here we only briefly outline the procedure followed.

Numerical simulations of the spectra were performed starting from the known geometric structures of *Rps. acidophila* and *Rsp. molischianum*. The magnesium atoms

TABLE 2 Fit parameters for the type 1 antenna systems

Parameter	*Rps. acidophila*	*Rps. palustris* (HL)	*Rps. cryptolactis* (HL)	*Cm. vinosum*
E800 (cm^{-1}; nm)	12531; 798	12500; 800	12500; 800	12500; 800
E850 (cm^{-1}; nm)	12195; 820	12195; 820	12195; 820	12165; 822
ΔE (cm^{-1})	300	300	300	300
ϵ	1.2	1.2	1.2	1.3
Δ (cm^{-1})	150	150	150	150
σ (cm^{-1})	450	450	450	450
B850$_\alpha$(z) (degrees)	7	7	7	7
B850$_\beta$(z) (degrees)	0	0	0	0
B800(x) (degrees)	0	3.5	6	7.5

E800: energy of the B800 pigments in cm^{-1} and absorption wavelength in nm. B850: mean energy of the B850 pigments in cm^{-1} and absorption wavelength in nm. ΔE: difference in excitation energy of the B850 α and B850 β pigments. ϵ: Relative dielectric constant of the surrounding medium, mainly a fit parameter to modify the interaction strength of the pigments. Δ: Homogeneous broadening FWHM; to account for the longer lifetime of the lowest excitonic state, we reduced the FWHM of that state by a factor of 50. σ: FWHM of a Gaussian distribution for diagonal disorder of the B850 pigments. The disorder of the B800 pigments was taken as half that of the B850 pigments to account for the smaller linewidths of the B800 spectra. B850$_\alpha$(z): angle over which the B850 α pigments were rotated around the pigment z-axis. B850$_\beta$(z): angle over which the B850 β pigments were rotated around the pigment z-axis. B800(x): angle of rotation of the B800 pigments around the pigment x-axis. Note that all rotations are in fact designed to move the Q_y transition moments closer to (for positive values) or further away from (for negative values) the plane of the ring. Angles are with respect to the angles determined from the PDB files, and all fits were performed on the full ring structures with 27 pigments.

were chosen as the center of the pigments, the direction of the Q_y transition moments were assumed to be parallel to the NB-ND direction, and the Q_x transition moments parallel to the NA-NC direction. Interaction energies between the chromophores were calculated in the point dipole approximation, and a relative dielectric constant of ~1.2 was used to account for the effect of the protein. As already indicated in the Introduction, this gives interaction energies consistent with experimental results, and also with a number of more sophisticated quantum chemical model calculations.

Although the consensus at the moment appears to be that interaction energies of around 300 cm^{-1} between nearest-neighbor pigments are of the correct order of magnitude, based both on experimental and theoretical data, considerably larger values are sometimes also reported (Linnanto et al., 1999). Although larger values of the interactions can contribute to the overall redshift of the antenna complex, as a consequence the high exciton component of the B850 ring moves far to the blue, where it cannot be observed due to overlap with other transitions. Because the B850 high exciton transition is almost coincident with the B800 contributions, modeling of the absorption and CD spectra can still be apparently successful. Since it was shown in Koolhaas et al. (1998) that the high exciton component of the B850 ring can be observed around 800 nm, the total width of the excitonic manifold does not support higher interaction energies than ≈300 cm^{-1}. In this paper we also show that the 800-nm CD spectrum can be understood as a combination of B800 and B850 high excitonic CD, again providing support for the magnitudes of the interaction energies used here.

The resulting Hamiltonian can then be diagonalized numerically, resulting in a stick spectrum. Inhomogeneous broadening was introduced by giving the diagonal elements

of the Hamiltonian a random contribution chosen from a Gaussian distribution of given width, and homogeneous broadening by convoluting each of the resulting sticks with a Gaussian, which is appropriate in the high temperature limit (Mukamel, 1995; Ch. 8). As was shown in Koolhaas et al. (2000), the difference between using homogeneous and inhomogeneous width is not distinguishable in linear spectroscopy, although the parameters (variances) are different because the inhomogeneous, diagonal disorder contribution leads to exchange narrowing, whereas homogeneous broadening does not.

As was indicated before, there are three parameters relevant for successful modeling of the absorption and CD spectrum. The first is the excitation energy difference between the α- and β-bound chromophores. The B850 ring can be viewed as a dimer of two rings (Koolhaas, 1999; Koolhaas et al., 2000), one consisting of the α-bound pigments, the other of the β-bound pigments. If we disregard disorder for a moment, each excitonic state $|k\rangle$ of the individual ring can be assigned a transition dipole moment $\boldsymbol{\mu}_k$ and a magnetization $\boldsymbol{m}_k$, which only for the lowest three excitonic states $k = 0, \pm1$ have nonzero values. The transition moments give the absorption spectrum: each line has an intensity proportional to μ_k^2, whereas the magnetization is responsible for the CD spectrum: each line has an intensity proportional to $\boldsymbol{\mu}_k \cdot \boldsymbol{m}_k$. In addition, it was shown that upon the coupling of these rings only states with the same k-value couple, so that only a simple dimer problem needs to be solved for each k-value. The interaction energy between the different k-states is dominated by the nearest-neighbor interaction of the pigments, and is therefore quite strong. The resulting CD spectrum has, of course, an excitonic contribution in addition to the individual magnetizations $\boldsymbol{m}_k$ (Cantor and Schimmel, 1980; Ch. 8), which have opposite signs for the excitonic states of the α- and β-bound pigment rings.

TABLE 3 Fit parameters for the type 2 antenna systems

Parameter	*Rsp. molischianum*	*Rb. sphaeroides*	*Ru. gelatinosus* (HL)
E800 (cm^{-1}; nm)	12579; 795	12547; 797	12500; 800
E850 (cm^{-1}; nm)	12180; 821	12300; 813	12285; 814
ΔE (cm^{-1})	300	300	300
ϵ	1.5	1.5	1.2
Δ (cm^{-1})	150	150	150
σ (cm^{-1})	400	400	400
B850$_{\alpha}$(z) (degrees)	7	7	7
B850$_{\beta}$(z) (degrees)	5	−10	−10
B800(x) (degrees)	0	4	13

Meaning of the symbols as in Table 2. The two *sphaeroides* strains are virtually identical, and are not separately reported. All simulations in this case were based on the *Rsp. molischianum* PDB file, with 24 pigments in the ring. In some cases the B800 homogeneous linewidth was slightly changed to get a better fit.

By changing the relative contributions of the two rings, which can easily be achieved by changing the excitation energies of the pigments in a ring, significant changes occur in the resulting CD spectrum, particularly the position of the zero crossing of the CD spectrum in the B850 band. The energy difference $E_{\alpha} - E_{\beta}$ needed is of the order of 300 cm^{-1}, and is probably the result of specific protein-pigment interactions. Quantum chemical calculations partially confirm this assumption (Alden et al., 1997).

The second parameter is the angle the Q_y transition dipoles make with the ring. Because the transition dipoles are almost in the plane of the ring for both the B800 and B850 pigments and for both structures, small changes lead to relatively large modifications of the resulting CD spectrum. The absorption spectrum is of course much less sensitive to those changes. The CD spectrum in the 800-nm region is to a large extent the combination of two weak contributions: the high exciton band of the B850 ring and the contribution of the weakly coupled B800 pigments. A change of only 7° can make the B800 CD vanish completely, and we will show that the measured behavior of the CD spectra in the 800-nm region can be explained very nicely by changing the relative contributions of the B850 high excitonic component and the B800 pigments, by changing the angle of the Q_y transition moments by only a few degrees.

The last parameter of relevance is the ratio of the interaction energy to the variance of homogeneous and inhomogeneous broadening. Large disorder tends to localize the excitations. Homogeneous broadening appears to have the same effect, but that is due to the overlap between the positive and negative contributions to the density of states (Koolhaas et al., 2000). Because we probe only the complete density of states with linear spectroscopies, the difference between those two mechanisms is not visible in the spectra. Because simulations with inhomogeneous broadening take considerably longer than those with just homoge-
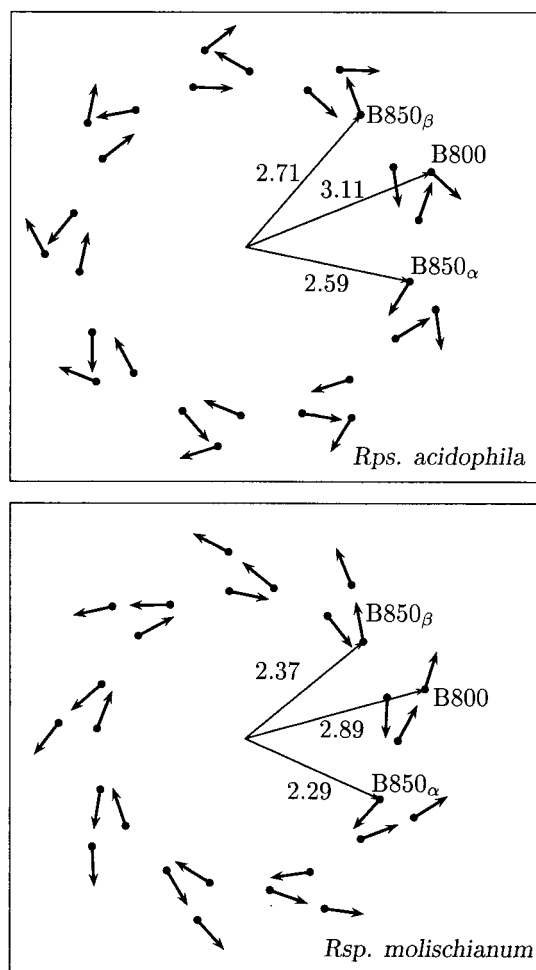

FIGURE 5 *Top:* Positions and orientations of the Q_y transition moments of *Rps. acidophila*, based on the Brookhaven Protein Data Bank structure 1KZU. Distances in nm. The angles the dipole moments make with the plane of the ring are −8.4° for the B800 pigments, −7.8° for the B850$_{\alpha}$, and −7.4° for the B850$_{\beta}$ pigments. The aggregate *z*-axis is chosen perpendicular to the ring, pointing toward the periplasmic side. This implies that the Q_y transition dipole moments point slightly downward from the plane, hence the negative angles. *Bottom:* Positions and orientations of the Q_y transition moments of *Rsp. molischianum*, based on the Brookhaven Protein Data Bank structure 1LGH. Distances in nm. The angles the dipole moments make with the plane of the ring are −12.5° for the B800 pigments, −7.2° for the B850$_{\alpha}$, and −7.0° for the B850$_{\beta}$ pigments. Note the opposite chirality of the B800 ring compared to that of the structure of *Rps. acidophila*. This is the origin of the different signatures of the CD spectra of the type 1 and type 2 species.

neous broadening, most simulations were first performed using homogeneous broadening only. After a reasonable fit was obtained, the inhomogeneous broadening was introduced by changing the appropriate parameters, accounting for exchange narrowing. Thus only a few full simulations needed to be performed.

Starting parameters to get a reasonable estimate of the interaction energies and line widths were obtained from the absorption spectra that are not very sensitive to changes in
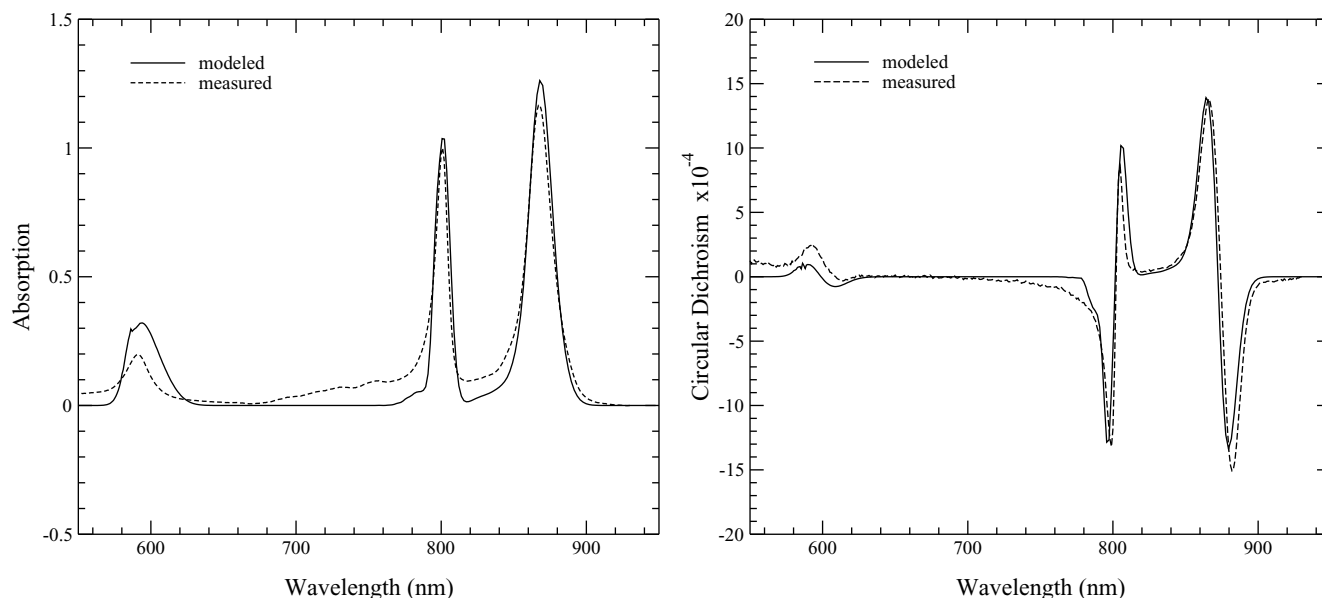
FIGURE 6 *Left:* Experimental (- - -) and calculated (——) absorption spectra of *Rps. acidophila*; *right:* experimental (- - -) and calculated (——) circular dichroism spectra of *Rps. acidophila*. The parameters used to calculate the spectra can be found in Table 2. In the calculations the Q_x transition was also included, without making any further changes to the structure. For the Q_x transition moment 1.9 D was used (Visschers et al., 1991), and the direction was chosen along the NA-NC axis in the pigments. The rotations performed to get a good fit of the $800-850$-nm spectrum also affect the direction of the Q_x moments. The calculated spectra and the experimental spectra were scaled to same value of the positive (blue) B850 CD line, as in the later figures.

the energy difference between α- and β-bound pigments, and the precise values of the angles of the transition dipoles with the ring plane. After that, varying the angles of the Q_y transition moments was sufficient to get good fits of the experimental spectra. The interaction energy between the pigments could be modified by taking the dielectric properties of the surrounding medium into account. The unmodified dipole-dipole interaction between the pigments gives an energy-splitting between the high- and low-energy components of the B850 band a little too large. Adding a reasonable dielectric constant of 1.2 reduces this interaction energy by 20%, which gives excellent agreement with the positions of the absorption peaks, where we assume, on the basis of the CD spectra, that the high exciton component of the B850 band is in fact overlapping the B800 absorption. It is noted here that our aim was not so much to get exact parameter values from the spectra, but rather to identify trends that can explain the differences between the spectra of a certain type.

The homogeneous broadening linewidth was taken to be 150 cm^{-1}, for each excitonic state, reflecting the short lifetimes (<100 fs) for those states. Only the lowest state was given a smaller linewidth, because it has a larger lifetime. Inhomogeneous broadening was varied to obtain a good fit. For the B800 pigments it was always taken at 0.2 the value of the B850 pigments. The rationale for this is that additional disorder is present in the B850 ring, due to the nearby presence of other pigments, and that the disorder in the interaction energies is not taken into account. Values of these parameters are also reported in Tables 2 and 3.

Using these simulations, it is shown that within a type (*Rps. acidophila* or *Rsp. molischianum*) the small differences between the spectra are mainly the result of small changes in the angles of the pigment transition moments with the ring plane. The two types are distinguished by their symmetry number, either ninefold symmetry for the *Rps. acidophila* type or eightfold for the *Rsp. molischianum* type, but the main cause of the differences is in the orientations of the B800 pigments, not the symmetry number itself.

Modeling results

The results of the modeling of the spectra are shown in Figs. $6-10$. For the type 1 species, the Brookhaven Protein Data Bank structure 1KZU, for LH2 of *Rps. acidophila* (Prince et al., 1997) was used as a starting point, whereas for the type 2 spectra we used the structure 1LGH (Koepke et al., 1996) of *Rsp. molischianum*. The directions of the Q_y transition moments of both structures are shown in Fig. 5, where we note that the B850 rings have virtually identical geometries, except for the symmetry number of the ring of course, but the orientations of the B800 pigments differ considerably. The crucial parameter for explaining the CD spectra is the angle the transition dipoles make with the plane of the ring. In all cases this angle is very small (cf. legend to Fig. 5). If the transition dipoles were exactly in the plane, the CD signal would vanish completely, so small changes in these angles can have considerable effects on the CD signal, both in the 800- and 850-nm region.

Although we should not put too much emphasis on the precise values of the parameters involved, we were able to get rather accurate fits of the experimental spectra. In Fig. 6 we show a fit for *Rps. acidophila*, together with the experimental spectrum. Although we did not put in an extra effort to fit the Q_x region, just taking that transition moment into account shows a very good reproduction of that part of the spectrum as well. All the other spectra from the type 1 group can easily be reproduced by slightly rotating the B800 pigments, as is shown in Fig. 7, *top*. Basically, the 800-nm spectrum is the result of an overlap of a negative contribution due to the B850 component, and a somewhat sharper feature, with both positive and negative contributions due to the B800 pigments. Especially when the B800 contribution becomes small (as for the larger angles of rotation), the presence of the high exciton component of the B850 ring becomes more visible in the CD spectrum. Similar results are shown in Fig. 7, *bottom* for the *Rsp. molischianum* type. Again, a good fit was obtained for *Rsp. molischianum* itself (Fig. 9), and the other spectra were generated by slight changes of the parameters used. The parameters used for all the type 1 and type 2 spectra are collected in Tables 2 and 3.

Changing the symmetry number alone does not dramatically alter the spectra, as is shown in Fig. 10. Here we just changed the number of $\alpha\beta$-heterodimers in the ring, without changing any other parameters. The changes in the spectra are basically the result of changing interaction energies due to the larger or smaller distances the pigments have. By also changing the ring size (or just reducing, or increasing the interaction strength), the changes in the spectra can be greatly reduced.

Again, we want to stress the extreme sensitivity of some of the spectra to the particular conditions the samples were prepared under. It is obvious from our modeling data that small changes in the angles of the pigments, sometimes not more than one or two degrees, led to considerable differences in the CD features. It is easy to envision such changes due to minor temperature differences or local effects of the detergent.

DISCUSSION AND CONCLUSIONS

The relation between geometric structure and electronic properties is not trivial. There is no direct relation between the spectrum of a pigment, or collection of pigments, and their geometry. This means that additional assumptions have to be made to calculate spectra. In our case this means determination of parameters such as excitation energies, magnitudes and directions of transition dipole moments, shielding factors (such as the dielectric constant), and (in)-homogeneous broadening values to calculate the spectrum. Nevertheless, we base all calculations on one model for a large number of species. This single model explains the
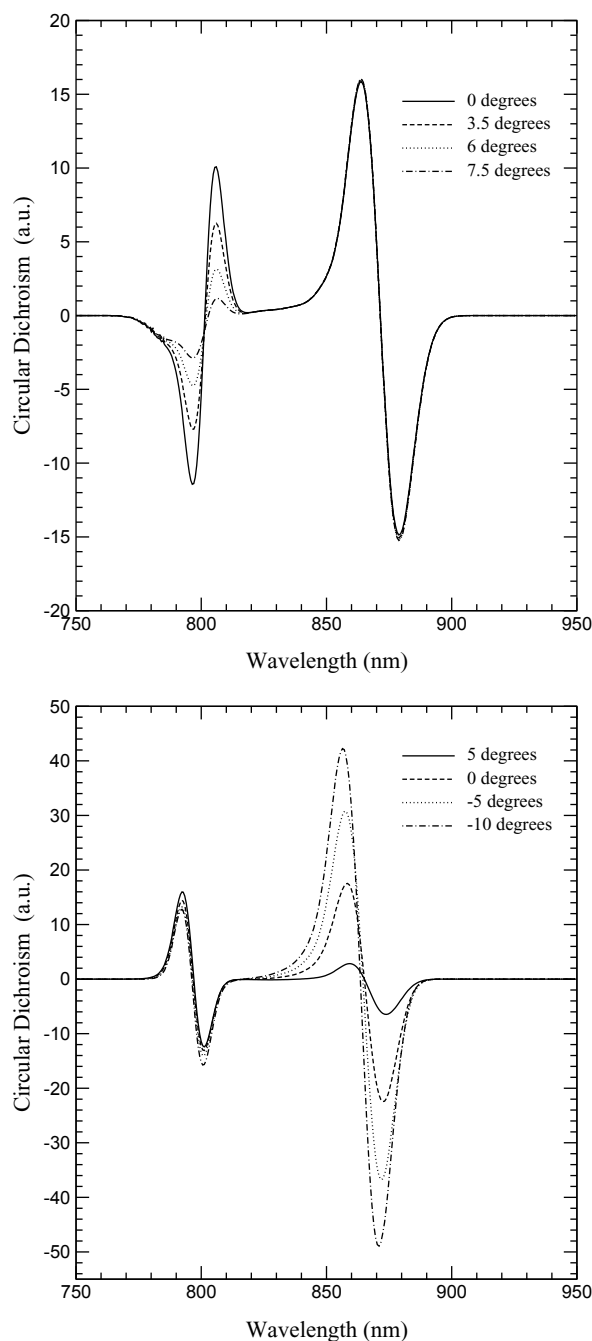

FIGURE 7 *Top:* Changes in the CD spectrum as a function of the angle of the B800 Q_y transition moments with the ring plane. The rotations were around the *x*-axis of the pigments, with a magnitude (highest to lowest peaks) of 0, 3.5, 6, and 7.5°, respectively. Because the original angle is −8.4°, a change of 7° makes the angle, and consequently the B800 CD almost vanish. The CD spectra of the type 1 LH2s can be thought to arise from such small changes. *Bottom:* Changes in the *Rsp. molischianum* spectrum upon rotation of the B850β pigments around their molecular *z*-axes. From the smallest to largest 850-nm CD the changes were 5, 0, −5, and −10°. Note that in the last two cases the dipoles were rotated further away from the ring plane, thus increasing the contribution of the β pigments to the CD spectrum.
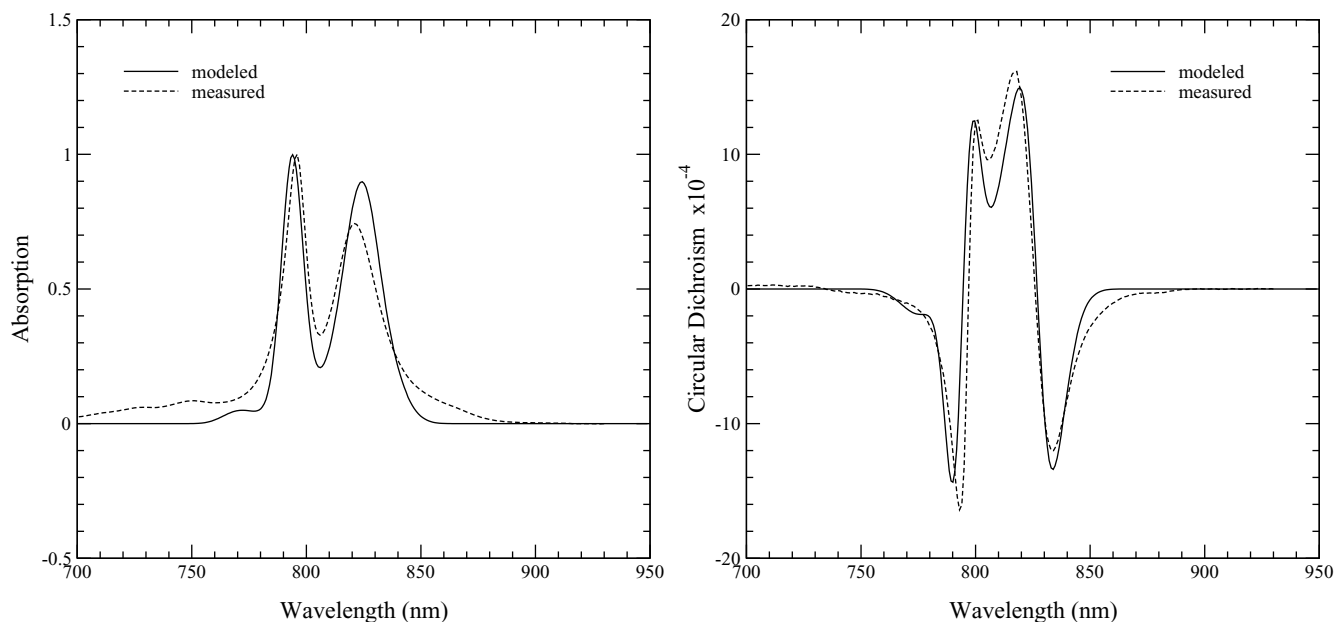
FIGURE 8 *Left:* Experimental (- - -) and calculated (—) absorption spectra of LL; *right:* CD spectra of *Rps. acidophila* (strain 7750). The fit parameters are the same as those for *Rps. acidophila* (strain 10050) except for the excitation energies, which were changed to 792 nm for the B800 energy and 795 nm for the mean energy of the B850 pigments, and the dielectric constant, which has a value of 2.0 in the simulation, which has the effect of much smaller interaction energies between the pigment. The large change in mean energy and in the dielectric constant both could reflect a major change in the direct environment of the pigments for this complex.

linear spectroscopic properties of a wide variety of species, at different temperatures, and under different conditions.

On the basis of this model we have shown that for a large number of different species, grown under different conditions, basically two types of LH2 antenna systems are formed: those with structures close to LH2 of *Rps. acidophila*, and those with structures close to *Rsp. molischianum*. We were able to explain most of the spectral features in the 800–850-nm region, where we put particular emphasis on the CD spectrum, in view of its sensitivity to small
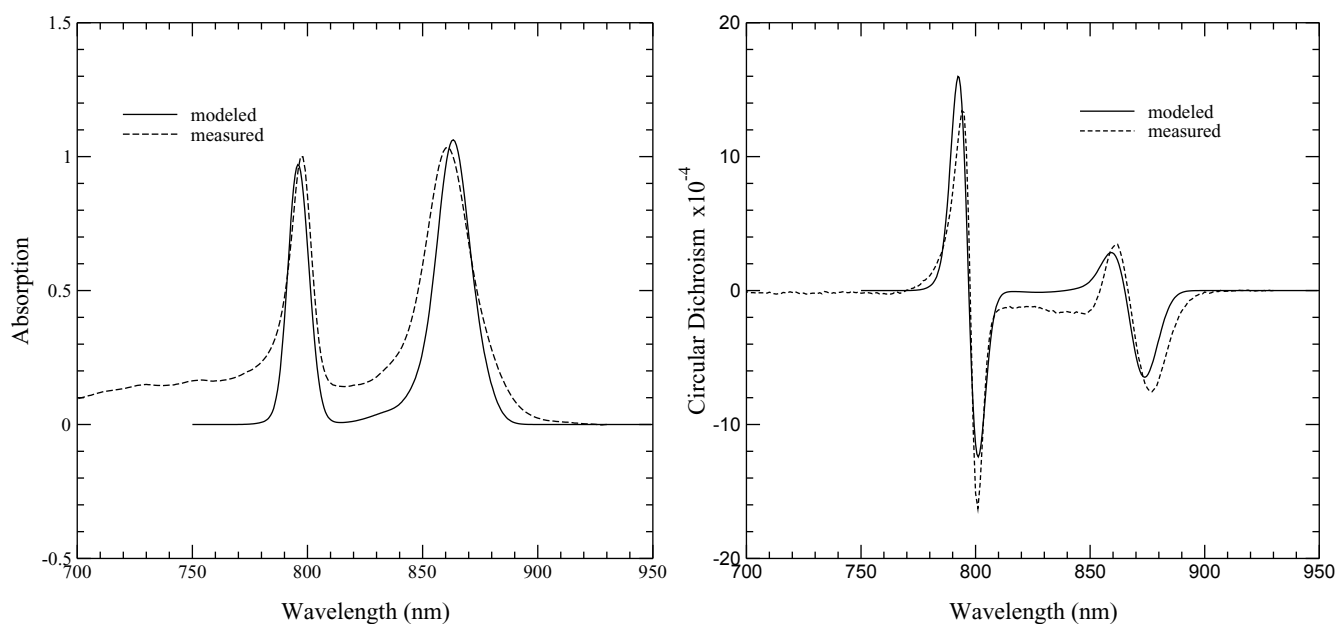

FIGURE 9 *Left:* Experimental (- - -) and calculated (—) absorption spectra of *Rsp. molischianum*; *right:* experimental (- - -) and calculated (—) circular dichroism spectra of *Rsp. molischianum*. Parameter values used are given in Table 3.
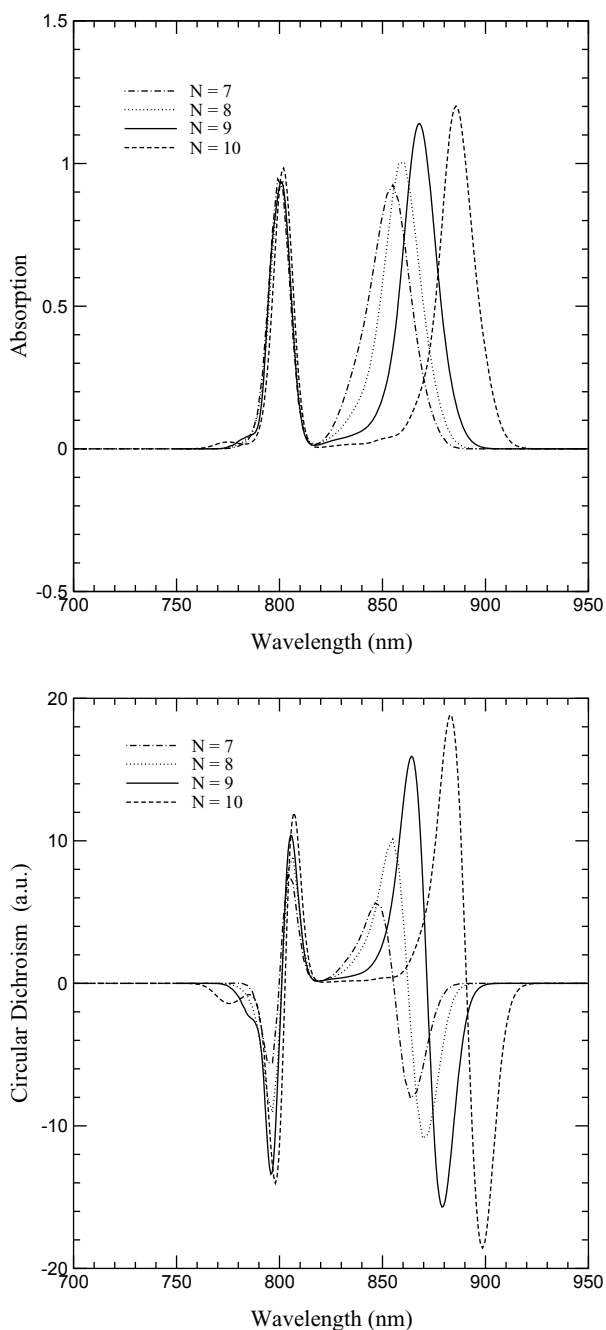
FIGURE 10 Changes in the absorption (*top*) and CD (*bottom*) spectrum for different values of the symmetry number. It is obvious that this change does not modify the signature of the CD spectrum. The major change is an increase (for larger *N*, or decrease (for smaller *N*) of the interaction energy. By increasing the ring size proportionally, that particular change can be undone. The figure is meant to indicate that merely changing the symmetry number is not sufficient to explain the differences between the two types of spectra.

changes in the angles the pigment transition moments make with the ring plane. This also shows that circular dichroism spectroscopy can be helpful in further refining structures, especially in cases where large cancellations occur, because

in those cases the spectra are extremely sensitive to small changes (Koolhaas et al., 1995, 1997b). In addition, this form of spectroscopy can also give some insight into the electronic structure of the pigments, albeit indirectly. Thus, the angles of the transition dipoles, although of course coupled to the geometry of the pigments, do not need to be parallel to the NB-ND or NA-NC directions, although they are likely to be close. Also, the excitation energy difference between the α- and β-bound pigments cannot be directly derived from the structure, although geometric deformations may play a role here (Alden et al., 1997).

The spectra are consistent with ring-like structures for all the species investigated. *Rb. sphaeroides* turns out to have a structure close to that of *Rsp. molischianum* (Jimenez et al., 1996; Walz et al., 1998), even though on the basis of our calculations we cannot rule out the possibility that the structure is a ring with ninefold symmetry. In fact, except for *Rsp. molischianum*, there is evidence from AFM microscopy data that some of the other systems are also ninefold ring structures, for instance *Ru. gelatinosus* (J.-L. Rigaud, personal communication). As is indicated below, modeling of the spectra can be done equally well with eight or ninefold rings, although this may mean minor adjustment of the interaction energies, for instance by modifying the dielectric constant.

The parameter sets that we determined from the spectra are not unique. There is a trade-off between the energy difference and the direction of the transition moments, which allows for other values of the parameters, although for an excitation energy difference below ≈ 200 cm^{-1}, no zero crossing of the B850 CD spectrum is found. Obviously, the directions of the Q_y transition moments have a certain amount of freedom; although it is believed that they are close to the NB-ND direction in the crystallized chromophores, in a protein environment these can easily change by a few degrees, due to static electric fields present in the protein (Gunner et al., 1996; Laberge et al., 1996; Phillips et al., 1999). This is, in fact, also a possible effect of off-diagonal disorder; due to the electric fields present in the environment the transition moment can acquire contributions from the static dipole moments, which can change the direction and magnitude of the transition moment (Van Mourik et al., 2001). Other forms of off-diagonal disorder can also contribute to changes in the direction of the transition moments, but it is important to realize that although we identify correlations between changes of the spectra and changes in the angles, we cannot identify causes for these changes, which may well come from changes in the environment. There is a lower limit for the energy difference between the α- and β-bound chromophores, below which the CD spectrum no longer exhibits a zero crossing around 860 nm. For the other parameters we have chosen to give values that allow a consistent change between the antenna systems of different species, and which appear to be reasonable in view of independent, quantum-chemical calcula-

tions. In addition, the spectra do not allow us to decide whether we are dealing with eight- or nine-membered rings. Although we have modeled the type 2 species with eight membered rings, there are indications that only *Rsp. molischianum* has an octamer of $\alpha\beta$-dimers, and all the other species consist of nine dimers. As our last figure indicates, this does not change the signature of the CD spectra, and in fact the calculated spectra in that figure can be made to overlap by changing the interaction strength, for instance by changing the dielectric constant.

REFERENCES

Aagaard, J., and W. R. Sistrom. 1972. Control of synthesis of reaction center bacteriochlorophyll in photosynthetic bacteria. *Photochem. Photobiol.* 15:209–225.

Alden, R. G., E. Johnson, V. Nagarajan, W. W. Parson, C. J. Law, and R. G. Cogdell. 1997. Calculations of spectroscopic properties of the LH2 bacteriochlorophyll-protein antenna complex from *Rhodopseudomonas acidophila. J. Phys. Chem. B.* 101:4667–4680.

Cantor, C. R., and P. R. Schimmel. 1980. Biophysical Chemistry. II. Techniques for the Study of Biological Structure and Function. W. H. Freeman and Company, San Francisco.

Clayton, R. K., and B. J. Clayton. 1981. B850 pigment-protein complex of *Rhodopseudomonas sphaeroides*: extinction coefficients, circular dichroism, and the reversible binding of bacteriochlorophyll. *Proc. Natl. Acad. Sci. U.S.A.* 78:5583–5587.

Cogdell, R. J., and A. R. Crofts. 1990b. Analysis of the pigment content of an antenna pigment/protein complex from three strains of *Rhodopseudomonas sphaeroides. Biochim. Biophys. Acta.* 502:409–416.

Cogdell, R. G., I. Durant, J. Valentine, J. G. Lindsay, and K. Schmidt. 1983. The isolation and partial characterisation of the light-harvesting pigment-protein complement of *Rps. acidophila. Biochim. Biophys. Acta.* 722:427–455.

Cogdell, R. J., and A. M. Hawthornthwaite. 1993. Preparation, purification and crystallization of purple bacterial antenna complexes. *In* The Photosynthetic Reaction Center, Vol. 1. J. R. Norris and J. Deisenhofer, editors. Academic Press, New York. 23–42.

Cogdell, R. J., A. M. Hawthornthwaite, M. B. Evans, L. A. Ferguson, C. Kerfeld, J. P. Thornber, F. van Mourik, and R. van Grondelle. 1990a. Isolation and characterisation of an unusual antenna complex from the marine purple sulphur photosynthetic bacterium *Chromatium purpuratum* BW5500. *Biochim. Biophys. Acta.* 1019:239–244.

Cogdell, R. G., and H. Scheer. 1985. Circular dichroism of light-harvesting complexes from photosynthetic bacteria. *Photochem. Photobiol.* 42:669–678.

Cogdell, R. J., and J. P. Thorber. 1979. The preparation and characterization of different types of light-harvesting pigment-protein complexes from some purple bacteria. *In* The CIBA Foundation Symposium 61(new series) on Chlorophyll Organisation and Energy Transfer in Photosynthesis. G. Wolstenholme and D. Fitzsimons, editors. Elsevier, Amsterdam. 61–79.

Cory, M. G., M. C. Zerner, X. Hu, and K. Schulten. 1998. Electronic excitations in aggregates of bacteriochlorophylls. *J. Phys. Chem. B.* 102:7640–7650.

Deisenhofer, J., O. Epp, O. Miki, R. Huber, and H. Michel. 1985. Structure of the protein subunits of the photosynthetic reaction centre of *Rhodopseudomonas viridis* at 3 Å resolution. *Nature.* 374:618–624.

Evans, M. B., A. M. Hawthornthwaite, and R. J. Cogdell. 1990. Isolation and characterization of the different B800–850 light harvesting complexes from low- and high-light grown cells of *Rhodopseudomonas cryptolactis. Biochim. Biophys. Acta.* 1016:71–76.

Freer, A. A., S. M. Prince, K. Sauer, M. Z. Papiz, A. M. Hawthornthwaite-Lawless, G. McDermott, R. J. Cogdell, and N. W. Isaacs. 1996. Pigment-pigment interactions and energy transfer in the antenna complex of the photosynthetic bacterium *Rhodopseudomonas acidophila. Structure.* 4:449–462.

Freiberg, A., A. Ellervee, P. Kukk, A. Laisaar, M. Tars, and K. Timpmann. 1994. Pressure effects on spectra of photosynthetic light-harvesting pigment-protein complexes. *Chem. Phys. Lett.* 214:10–16.

Frese, R. N., J. D. Olsen, R. Branval, W. H. J. Westerhuis, C. N. Hunter, and R. van Grondelle. 2000. The long-range supraorganization of the bacterial photosynthetic unit: a key role for PufX. *Proc. Natl. Acad. Sci. U.S.A.* 97:5197–5202.

Gunner, M., A. Nicholls, and B. Honig. 1996. Electrostatic potentials in *Rhodopseudomonas viridis* reaction centers: implications for the driving force and directionality of electron transfer. *J. Phys. Chem.* 100: 4277–4291.

Halloren, E., G. McDermott, J. G. Lindsay, C. Miller, A. A. Freer, N. W. Isaacs, and R. J. Cogdell. 1995. Studies on the light-harvesting complexes from the thermotolerant purple bacterium *Rhodopseudomonas cryptolactis. Photosynth. Res.* 44:149–155.

Hu, X., T. Ritz, A. Damjanović, and K. Schulten. 1997. Pigment organization and transfer of electronic excitation in the photosynthetic unit of purple bacteria. *J. Phys. Chem. B.* 101:3854–3871.

Iwata, S., J. W. Lee, K. Okada, J. K. Lee, M. Iwata, B. Rasmussen, T. A. Link, S. Ramaswami, and B. K. Jap. 1998. Complete structure of the 11-subunit bovine mitochondrial cytochrome bc_1 complex. *Science.* 281:64–71.

Jimenez, R., S. N. Dikshit, S. E. Bradforth, and G. R. Fleming. 1996. Electronic excitation transfer in the LH2 complex of *Rhodobacter sphaeroides. J. Phys. Chem.* 100:6825.

Jungas, C., J.-L. Ranck, J.-L. Rigaud, and A. Vermeglio. 1999. Supramolecular organization of the photosynthetic apparatus of *Rhodobacter sphaeroides. EMBO J.* 18:534–542.

Karrasch, S., P. Bullough, and R. Ghosh. 1995. The 8.5 Å projection map of the light-harvesting complex I from *Rhodospirillum rubrum* reveals a ring composed of 16 subunits. *EMBO J.* 14:631–681.

Koepke, J., X. Hu, C. Muenke, K. Schulten, and H. Michel. 1996. The crystal structure of the light harvesting complex II (B800–850) from *Rhodospirillum molischianum. Structure.* 4:581–597.

Koolhaas, M. H. C., G. van der Zwan, F. van Mourik, and R. van Grondelle. 1997b. Spectroscopy and structure of bacteriochlorophyll dimers. I. Structural consequences of non-conservative CD spectra. *Biophys. J.* 72:1828–1841.

Koolhaas, M. H. C. 1999. The Relation between the Structure and the Spectroscopy of Bacterial Light Harvesting Antennae. Ph.D. thesis, Vrije Universiteit, Amsterdam.

Koolhaas, M. H. C., R. N. Frese, G. J. S. Fowler, T. S. Bibby, S. Georgakopoulou, G. van der Zwan, C. N. Hunter, and R. van Grondelle. 1998. Identification of the upper exciton component of the B850 bacteriochlorophylls, using a B800-minus mutant of *Rhodobacter sphaeroides. Biochemistry.* 37:4693–4698.

Koolhaas, M. H. C., G. van der Zwan, R. N. Frese, and R. van Grondelle. 1997a. Red shift of the zero crossing in the CD spectra of the LH2 antenna complex of *Rhodopseudomonas acidophila*: a structure based study. *J. Phys. Chem. B.* 101:7262–7270.

Koolhaas, M. H. C., G. van der Zwan, and R. van Grondelle. 2000. Local and nonlocal contributions to the linear spectroscopy of light-harvesting antenna systems. *J. Phys. Chem. B.* 104:4489–4502.

Koolhaas, M. H. C., G. van der Zwan, F. van Mourik, and R. van Grondelle. 1995. Correlation of non-conservative CD signals, absorption spectra and dimer structure. Application to the B820 subunit. *In* Xth International Photosynthesis Congress. R. Matthis, editor. Kluwer Academic Publishers, The Netherlands. 351–354.

Krueger, B. P., G. D. Scholes, and G. R. Fleming. 1998. Calculation of couplings and energy transfer pathways between the pigments of LH2 by

the ab initio transition density cube method. *J. Phys. Chem. B.* 102: 5378–5386.

Laberge, M., J. M. Vanderkooi, and K. A. Sharp. 1996. Effect of a protein electric field on the CO stretch frequency. finite difference Poisson-Boltzmann calculations on carbonmonoxycytochromes. *J. Phys. Chem. B.* 100:10793–10801.

Linnanto, J., J. E. I. Korppi-Tommola, and V. M. Helenius. 1999. Electronic states, absorption and CD spectra of the photosynthetic bacterial LH2 antenna of *Rhodopseudomonas acidophila* as predicted by exciton theory and semi-empirical calculations. *J. Phys. Chem. B.* 103: 8739–8750.

McDermott, G., S. M. Prince, A. A. Freer, A. M. Hawthornthwaite-Lawless, M. Z. Papiz, R. J. Cogdell, and N. W. Isaacs. 1995. Crystal structure of an integral membrane light harvesting complex from photosynthetic bacteria. *Nature.* 374:517–521.

Monshouwer, R., M. Abrahamson, F. van Mourik, and R. van Grondelle. 1997. Superradiance and exciton delocalization in bacterial photosynthetic light-harvesting systems. *J. Phys. Chem. B.* 101:7241–7248.

Mukamel, S. 1995. Principles of Nonlinear Optical Spectroscopy. Oxford University Press, New York.

Novoderezhkin, V. I., R. Monshouwer, and R. van Grondelle. 1999. Exciton (de)localization in the LH2 antenna of *Rhodobacter sphaeroides* as revealed by relative difference absorption measurements of the LH2 antenna and the B820 subunit. *J. Phys. Chem. B.* 103:10540–10548.

Phillips, G. N., Jr., M. L. Teodoro, T. Li, B. Smith, and J. S. Olson. 1999. Bound CO is a molecular probe of electrostatic potential in the distal pocket of myoglobin. *J. Phys. Chem. B.* 103:8817–8829.

Prince, S. M., M. Z. Papiz, A. A. Freer, G. McDermott, A. M. Hawthornthwaite-Lawless, R. J. Cogdell, and N. W. Isaacs. 1997. Apoprotein structure in the LH2 complex from *Rhodopseudomonas acidophila* strain 10050: modular assembly and protein-pigment complexes. *J. Mol. Biol.* 268:412–423.

Pullerits, T., M. Chachisvilis, and V. Sundström. 1996. Exciton delocalization length in the B850 antenna of LH2 of *Rhodobacter sphaeroides*. *J. Phys. Chem.* 100:10787–10792.

Pullerits, T., and V. Sundström. 1996. Photosynthetic light-harvesting pigment-protein complexes: toward understanding how and why. *Acc. Chem. Res.* 29:381–390.

Rätsep, M., H.-M. Wu, J. M. Hayes, R. E. Blankenship, R. J. Cogdell, and G. J. Small. 1998. Stark hole-burning studies of three photosynthetic complexes. *J. Phys. Chem. B.* 102:4035–4044.

Reddy, N. R. S., G. J. Small, M. Seibert, and R. Picorel. 1991. Energy transfer dynamics of the B800–B850 antenna complex of *Rhodobacter sphaeroides*: a hole burning study. *Chem. Phys. Lett.* 181:391–399.

Sauer, K., R. J. Cogdell, S. M. Prince, A. A. Freer, N. W. Isaacs, and H. Scheer. 1996. Structure-based calculations of the optical spectra of LH2 bacteriochlorophyll-protein complex from *Rhodopseudomonas acidophila*. *Photochem. Photobiol.* 64:564–576.

Scholes, G. D., I. R. Gould, R. J. Cogdell, and G. R. Fleming. 1999. Ab initio molecular orbital calculations of electronic couplings in the LH2 bacterial light-harvesting complex of *Rps. acidophila. J. Phys. Chem.* 103:2543–2553.

Shinkarev, V. P., and C. A. Wraight. 1993. Electron and proton transfer in the acceptor quinone complex of reaction centers of phototropic bacteria. *In* The Photosynthetic Reaction Center. J. Deisenhofer and J. R. Norris, editors. Academic Press, Inc., San Diego. 194–255.

Sundström, V., T. Pullerits, and R. van Grondelle. 1999. Photosynthetic light-harvesting: reconciling dynamics and structure of purple bacterial LH2 reveals function of photosynthetic unit. *J. Phys. Chem. B.* 103: 2327–2346.

Tharia, H. A., T. D. Nightingale, M. Z. Papiz, and A. M. Lawless. 1999. Characterization of hydrophobic peptides by RP-HPLC from different spectral forms of LH2 isolated from *Rps. palustris. Photosynth. Res.* 61:157–167.

Tretiak, S., V. Chernyak, and S. Mukamel. 2000. Bacteriochlorophyll and carotenoid couplings in the LH2 system of purple bacteria. *J. Phys. Chem. B.* 104:9540–9553.

Van Grondelle, R., P. Dekker, T. Gillbro, and V. Sundstrom. 1994. Energy transfer and trapping in photosynthesis. *Biochim. Biophys. Acta.* 1187: 1–65.

Van Mourik, F., M. Chergui, and G. van der Zwan. 2001. The occurrence of non-Gaussian spectral line-shapes of molecules in electrostatically disordered media. *J. Phys. Chem. B.* 105:9715–9718.

Visschers, R. W., M. C. Chang, F. van Mourik, P. S. Parkes-Loach, B. A. Heller, P. A. Loach, and R. van Grondelle. 1991. Fluorescence polarization and low-temperature absorption spectroscopy of a subunit form of light-harvesting complex I from purple photosynthetic bacteria. *Biochemistry.* 30:5734–5742.

Walz, T., S. J. Jamieson, C. M. Bowers, P. A. Bullough, and C. N. Hunter. 1998. Projection structures of three photosynthetic complexes from *Rhodobacter sphaeroides*: LH2 at 6 Å, LH1 and RC-LH1 at 25 Å. *J. Mol. Biol.* 282:833–845.

Wu, H.-M., M. Rätsep, R. Jankowiak, R. J. Cogdell, and G. J. Small. 1997. Comparison of the LH2 antenna complexes of *Rhodopseudomonas acidophila* (strain 10050) and *Rhodobacter sphaeroides* by high pressure-absorption, -hole burning and temperature-dependent absorption spectroscopy. *J. Phys. Chem. B.* 101:7641–7653.

Xia, D., C.-A. Yu, H. Kim, J. Z. Xia, A. M. Kachurin, L. Yu, and J. Deisenhofer. 1977. Crystal structure of the cytochrome bc_1 complex from bovine heart mitochondria. *Science.* 277:60–66.

Zuber, H., and R. J. Cogdell. 1995. Structure and organization of purple bacterial antenna complexes. *In* Advances in Photosynthesis, Vol. 2. Anoxygenic Photosynthetic Bacteria. R. E. Blankenship, M. T. Madigan, and C. E. Bauer, editors. Kluwer Academic Publishers, Dordrecht, The Netherlands.